Infrared Physics & Technology 90 (2018) 66–69

Contents lists available at ScienceDirect

Infrared Physics & Technology

journal homepage: www.elsevier.com/locate/infrared

Regular article

Far-infrared study of the mechanochemically synthesized Cu_2FeSnS_4 (stannite) nanocrystals

J. Trajic [a,*], M. Romcevic [a], N. Paunovic [a], M. Curcic [a], P. Balaz [b], N. Romcevic [a]

[a] Institute of Physics, University of Belgrade, 11080 Belgrade, Serbia
[b] Institute of Geotechnics, Slovak Academy of Sciences, 043 53 Kosice, Slovakia

HIGHLIGHTS

- Stannite Cu_2FeSnS_4 nanocrystals were synthesized mechanochemically.
- Optical properties and compositional purity of Cu_2FeSnS_4 nanocrystals were characterized.
- Optical properties were investigated by Far-infrared spectroscopy.
- The influence of the milling time on synthesis of the stannite Cu_2FeSnS_4 was observed.

GRAPHICAL ABSTRACT

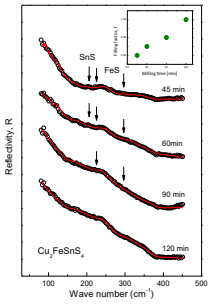

ARTICLE INFO

Article history:
Received 25 December 2017
Revised 22 February 2018
Accepted 22 February 2018
Available online 23 February 2018

Keywords:
Nanostructures
Optical properties
Far-infrared spectroscopy

ABSTRACT

The analysis of the optical properties of mechanochemically synthesized stannite Cu_2FeSnS_4 nanocrystals has been performed using far-infrared spectroscopy. The Cu_2FeSnS_4 stannite nanocrystals were synthesized mechanochemically from elemental precursors Cu, Fe, Sn, and S. Milling time was 45, 60, 90 and 120 min. Reflectivity spectra were analyzed using the classical form of the dielectric function, which includes the phonon and the free carrier contribution. The influence of milling time on synthesis of stannite Cu_2FeSnS_4 is observed. Among the modes that are characteristic for the stannite Cu_2FeSnS_4, we registered the modes of binary phases of FeS and SnS. The total disappearance of the binary phases of FeS and SnS and forming pure Cu_2FeSnS_4 is observed when the milling time is 120 min. Effective permittivity of Cu_2FeSnS_4 and binary phases of FeS and SnS were modeled by Maxwell – Garnet approximation.

1. Introduction

Stannite (Cu_2FeSnS_4) is one of the best-known sulphide minerals, not only because of its economic importance as a tin ore, but also because of its structural and physical characteristics [1] such as adequate direct band gap (1.0–1.5 eV), low toxicity and a relatively high abundance of the elements in the Earth's crust [2]. Its constituents are abundantly available [3].

To deal with the increasingly severe energy crisis, research on high-efficient and low-cost solar cells is of pressing need and of great significance. Various types of semiconductors such as CdTe, $Cu(In,Ga)Se_2$ and TiO_2, have been extensively studied for thin film solar cells. Nevertheless, due to the toxicity of Cd and the limited availability of In and Ga, naturally abundant and non-toxic photo-voltaic materials are of considerable interest [4]. Quaternary semiconductor Cu_2FeSnS_4 is one of promising photovoltaic materials as an alternative absorber layer for the development of low-cost and environment-friendly thin film solar cells due to its analogous crystal structures to $Cu(In,Ga)Se_2$, suitable band gap and high absorption coefficient [5].

Several low-cost, highly efficient, environmental friendly and easy-to operate methods have been developed for preparation of Cu_2FeSnS_4, such as pulse laser and electro deposition [6], hot

* Corresponding author.
E-mail address: jelena@ipb.ac.rs (J. Trajic).

https://doi.org/10.1016/j.infrared.2018.02.010
1350-4495/

injection [7], electrospinning [8], dip coating [9], microwave assisted approach [4,10,11] and oxide-nanoparticles-based process [12]. However, these techniques are complex as well as time-consuming, and require high temperature, while in some cases it is necessary to use the toxic organic solvents. Mechanochemical treatment is a powerful technique for synthesis of a wide range of materials where the high energy milling is being applied to induce and speed up chemical reactions [13,14]. This approach is simple, solvent-free, and reproducible, and also the synthesis might be easily scaled up. However, the control of stoichiometry and crystal structure during synthesis of the quaternary nanocrystals remains a challenge.

In this paper, the optical and structural properties of Cu_2FeSnS_4 nanoparticles which are mechanochemically synthesized have been investigated using far-infrared spectroscopy. The reflectivity spectra of the tetragonal Cu_2FeSnS_4 obtained after different milling time have been analyzed using the Maxwell–Garnett approximation. We have determined the influence of the milling time on the purity of the Cu_2FeSnS_4 nanocrystals.

2. Samples preparation and characterisation

The elemental precursors (Cu, Fe, Sn and S) were used to obtain stannite (CFTS) by a solid state one-pot mechanochemical synthesis. The starting materials were elemental Cu (99%), Fe (99%), Sn (99.9%), and S (99%). These materials were weighed and mixed in atomic ratios of 2:1:1:4, according to the stoichiometry Cu_2FeSnS_4. The particularities of synthesis and initial characterization of Cu_2FeSnS_4 nanoparticles were presented previously in Refs. [15,16], and will be briefly discussed here.

The mechanochemical synthesis of Cu_2FeSnS_4 nanoparticles was performed in a Pulverisette 6 planetary mill (Fritsch, Germany). The milling conditions were as follows: milling pot volume-250 ml, material of milling pot – tungsten carbide (WC) with 50 WC balls of 10 mm diameter in it, total weight of reactants – 5 g, ball-to-powder mass ratio – 70, milling speed – 500 min^{-1}. Milling time was 45, 60, 90 and 120 min using an argon protective atmosphere in the mill. Using the described synthesis process, the unique nanostructures and properties are developed. Cu_2FeSnS_4 polymorphs with tetragonally body-centred structure with crystallite sizes of 18–19 nm were obtained.

X-ray diffraction (XRD) is the most commonly used technique to characterize the crystal structure and compositional purity of stannite Cu_2FeSnS_4 nanoparticles. All samples were examined under the same conditions, using a D8 Advance Bruker X-ray diffractometer in the Bragg-Brentano geometry, using the Cu Kα radiation of 0.15418 nm and a scintillation detector at room temperature. The commercial Bruker tools have been used for data processing.

The XRD patterns of the elemental mixture (Cu, Fe, Sn and S powders) obtained after various milling times are shown in the Fig. 1. Diffraction patterns show the reflection of the tetragonal body-centred stannite Cu_2FeSnS_4 according to card JCPDS 44-1476 in the tetragonal space group *I*-42*m*. The XRD spectra shows three most intensive peaks at $2\theta = 28.5°$, 47.5° and 56.0° that can be assigned to the (1 1 2), (2 0 4), and (3 1 2) planes of the tetragonal crystals. Besides mentioned peaks, the peak of the Fe is observed at the Cu_2FeSnS_4 nanocrystal samples obtained after 45 and 60 min milling time. This peak disappears with increasing milling time.

In the attempt to characterize compositional purity of stannite, and observe the influence of the milling time on the mechanochemical synthesis of Cu_2FeSnS_4 nanocrystals we used far-infrared (FIR) spectroscopy. The infrared reflectivity measurements were carried out at room temperature with a BOMEM DA-8 Fourier-transform IR spectrometer. A deuterated triglycine sulfate (DTGS) pyroelectric detector was used to cover the wave number region from 80 to 450 cm^{-1}.

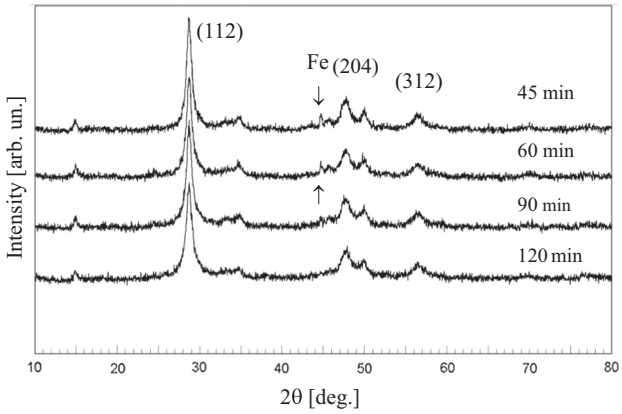

Fig. 1. XRD spectra of Cu_2FeSnS_4 nanocrystals obtained after various milling times.

3. Results and discussion

The Cu_2FeSnS_4 is a tetrahedrally coordinated semiconductor in which each sulphur anion is bonded to four cations and each cation is bonded to four sulphur anions [17]. The factor group analysis of the allowed zone-centre vibrations for the *I*-42*m* tetragonal crystallographic structures of Cu_2FeSnS_4, indicates that ten infrared (IR) and fourteen Raman active phonon modes of irreducible representations are expected for this compound [18]:

$$\Gamma = 2A_1 + A_2 + 2B_1 + 4B_2 + 6E \quad (1)$$

The B_2 and E modes are IR active and they represent LO-TO splitting due to their polar character. The modes A_1, B_1, B_2 and E are Raman active.

Reflectivity spectra were analyzed using the classical form of the dielectric function, which includes several oscillators and the free carrier contribution to the dielectric function [19]. Whereas the analysis of the far IR reflectivity spectrum of Cu_2FeSnS_4 nanopowders revealed a presence of a plasmon mode, it was necessary to include both contributions of the phonon and the plasmon (free carrier contribution) to the dielectric function:

$$\varepsilon_s(\omega) = \varepsilon_\infty \left(\sum_{j=1}^{l} \frac{\omega_{LOk}^2 - \omega^2 + i\gamma_{LOk}\omega}{\omega_{TOk}^2 - \omega^2 + i\gamma_{TOk}\omega} - \frac{\omega_{P2}}{\omega(\omega + i\Gamma_P)} \right) \quad (2)$$

where ε_∞ is the high-frequency dielectric constant, ω_{LOk}, and ω_{TOk} are longitudinal and transverse frequencies of the *k*-th oscillator, γ_{LOk} and γ_{TOk} are their corresponding dampings, ω_p and Γ_p are the plasma frequency and damping. The first term in Eq. (2) is the lattice contribution whereas the second term is the Drude expression for the free carrier contribution to the dielectric constant. The far-infrared reflection spectrum of Cu_2FeSnS_4 nanocrystal obtained after 45 min milling time is presented in Fig. 2. The experimental data are presented by circles, while the solid line represents the calculated reflectivity spectra obtained by the fitting procedure based on Eq. (2). In the fitting procedure we included modes at about 93, 120, 144, 250, 315 and 350 cm^{-1} that are in accordance with the reported values for tetragonal Cu_2FeSnS_4 [18,20] as well as, plasma term. We did not succeed to determinate the set of parameters that provide good spectrum overlapping in the whole range of frequencies. Discrepancy between experimental and calculated reflectivity spectra in some regions is obvious,

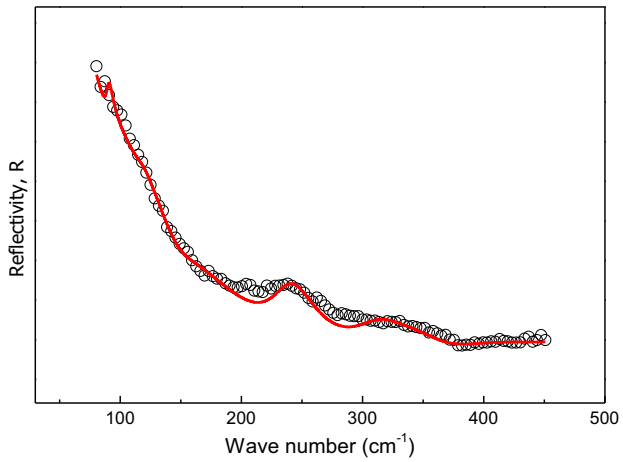

Fig. 2. Far-infrared reflection spectra of stannite Cu_2FeSnS_4 obtained after 45 min milling time. Experimental spectra are presented by circles. The solid lines are calculated spectra obtained by a fitting procedure based on the model given by Eq. (2).

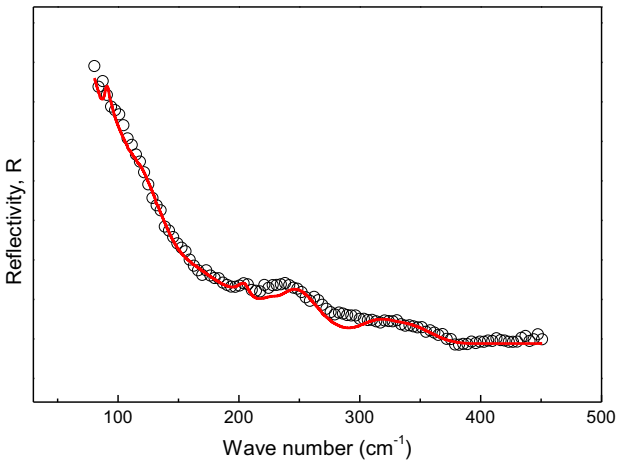

Fig. 3. Far-infrared reflection spectra of stannite Cu_2FeSnS_4 obtained after 45 min milling time. Experimental spectra are presented by circles. The solid lines are calculated spectra obtained by a fitting procedure based on the model given by Eq. (3).

which indicates that in this system among the nanocrystals of Cu_2FeSnS_4 exists another mixtures of starting elements and their phases.

Because our sample consists of Cu_2FeSnS_4 nanoparticles and binary and/or ternary phases of starting elements we have applied the effective medium approximation method to calculate infrared reflectivity spectra. The widely used effective medium theory is the Maxwell–Garnett approximation which treats the effective medium as consisting of a matrix in which are embedded inclusions and where the fraction of the inclusions is very small, so that the inclusions are spatially separated and can be treated as a perturbation [21,22]. For the spherical inclusions case, the prediction of the effective permittivity of mixture ε_{eff} according to the Maxwell-Garnet mixing rule reads [23,24]:

$$\varepsilon_{ff} = \varepsilon_1 + 3f\varepsilon_1 \frac{\varepsilon_2 - \varepsilon_1}{\varepsilon_2 + 2\varepsilon_1 - f(\varepsilon_1 - \varepsilon_2)} \quad (3)$$

Here, spheres of permittivity ε_2 are located randomly in homogeneous environment ε_1 and occupy a volume fraction f. In the case of mechanochemicaly sintesized Cu_2FeSnS_4, multicomponent phases of starting elements with dielectrical function ε_2 are randomly located in pure Cu_2FeSnS_4 with dielectrical function ε_1, where ε_1 and ε_2 are defined by Eq. (2).

In Fig. 3 is presented the far-infrared reflection spectrum of Cu_2FeSnS_4 nanocrystal obtained after 45 min milling time where the solid line is obtained by applying Maxwell–Garnett approximation. In the fitting procedure, besides modes which originated from tetragonal Cu_2FeSnS_4 we included mode at about 215 cm^{-1} which is corresponding to infrared frequency of SnS binary component [25]. Occurrence of SnS binary phase is in accordance with the observation of Bernardini et al, where, by thermal synthesis, also, the minor traces of herzenbergite SnS have been detected, besides stannite [1,26].

Taking into account this mode, corresponding to infrared frequency of SnS binary component, we obtained better overlapping, but it is obvious that besides binary phase of SnS the other multicomponent phases are formed. Satisfactory overlapping of experimental and theoretical spectra is achieved when in the fitting procedure the modes at about 225 and 297 cm^{-1} (Fig. 4a) are added. These two modes are originated from impurity FeS binary phases [17,27]. Slight difference in frequencies between available literature data as well as data we gathered probably arises from the differences in the cation-anion bond distances. Also, disordered

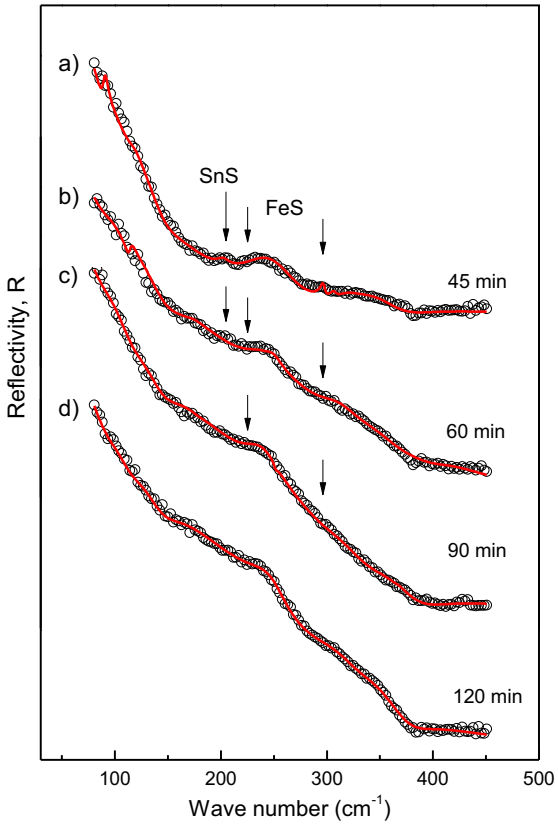

Fig. 4. Far-infrared reflection spectra of stannite Cu_2FeSnS_4 obtained after different milling times. Experimental spectra are presented by circles. The solid lines are calculated spectra obtained by a fitting procedure based on the model given by Eq. (3).

distribution of Cu and Fe atoms leads to the presence of a high content of Cu_{Fe} and Fe_{Cu} anti-site defects that would degrade the crystalline quality of these regions. The existence of a highly disordered distribution of cations in these domains would lead to a shift of the peak towards lower frequencies [28].

The far-infrared reflection spectra of Cu_2FeSnS_4 nanocrystals obtained after various milling times, in the spectral range from 80 to 450 cm^{-1}, are presented in Fig. 4. The experimental data

Table 1
Volume fraction of tetragonal Cu_2FeSnS_4 as a function of milling time.

Milling time [min]	Filling factor, *f*
45	0.96
60	0.97
90	0.98
120	1

are presented by circles, while the solid line represent the calculated reflectivity spectra obtained by the fitting procedure based on Eq. (3).

The spectrum of Cu_2FeSnS_4 nanocrystals obtained after 60 min milling time is presented in Fig. 4b. In the case of this nanocrystal the same modes are registered as in the sample obtained after 45 min milling time. Namely, modes originated from tetragonal Cu_2FeSnS_4, together with modes originated from binary phases FeS and SnS are registered at infrared spectra samples obtained after 45 and 60 min milling time. In infrared spectrum of sample obtained after 90 min milling time (Fig. 4c), the mode that corresponds to SnS was not observed, whereas in the case of the nanocrystal obtained after 120 min milling time (Fig. 4d), only the modes originated from pure tetragonal Cu_2FeSnS_4 are registered. This spectrum, obtained after 120 milling time, is calculated with the set of parameters corresponding to the pure Cu_2FeSnS_4 sample.

The total disappearance of the mode originated from SnS binary phase is observed after 60 min milling time, and FeS modes disappear when the milling time is 120 min (longer than 90 min). Absence of those modes excluded the presence of FeS and SnS binary phases, which indicates that after 90 min milling time pure stannite Cu_2FeSnS_4 is synthesized.

Volume fraction of tetragonal Cu_2FeSnS_4 obtained as estimation of the best fit parameter are presented in Table 1. As milling time increases, the filling factor increase also, which indicates that during miling the contribution of impurity binary phases FeS and SnS decrease, while contribution of pure, tetragonal Cu_2FeSnS_4 increases. Namely, Cu_2FeSnS_4 is synthesized from elemental precursors Cu, Fe, Sn and S by applying the high-energy milling. During synthesis besides tetragonal Cu_2FeSnS_4 nanocrystal the binary phases of starting elements FeS and SnS occur. In our case where the multicomponent phases of starting elements are randomly located in Cu_2FeSnS_4, the filling factor *f* gives us information about the contribution (volume fraction) of pure Cu_2FeSnS_4.

4. Conclusion

We have measured the far-infrared reflectivity spectra of the mechanochemically synthesized Cu_2FeSnS_4 nanocrystals obtained after different milling time. Reflectivity spectra were analyzed using the classical form of the dielectric function, which includes the phonon and plasmon contribution to the dielectric function. The best fit spectra are obtained using the Maxwell–Garnett approximation. Besides modes which are characteristic for tetragonal Cu_2FeSnS_4 nanocrystals we registered the existence of modes that originates from binary phases of FeS and SnS. The total disappearance of the mode originated from SnS binary phase is observed after 60 min milling time, and FeS modes disappear when the milling time is longer than 90 min. Absence of those modes excluded the presence of FeS and SnS binary phases, which indicates that after 90 min milling time pure stannite Cu_2FeSnS_4 is synthesized. As a best fit parameter we determined volume fraction of tetragonal Cu_2FeSnS_4 as a function of milling time. Analyzing the reflectivity spectra we determine not only which impurity components occur during the synthesis of Cu_2FeSnS_4, and we find out the change in contribution of these impurity components as the miling time is varied.

Acknowledgements

This work in Serbia was supported by Serbian Ministry of Education, Science and Technological Development under Project III45003. This work was also supported by Slovak Research and Developing agency (Project APVV – 14-0103).

Conflict of interest

None.

References:

[1] G.P. Bernardini, D. Borrini, A. Caneschi, F. Di Benedetto, D. Gatteschi, S. Ristori, M. Romanelli, Phys. Chem. Miner. 27 (2000) 453–461.
[2] B. Zhou, X. Yan, P. Li, L. Yang, D. Yu, Eur. J. Inorgan. Chem. 1 (2015) 2690–2694.
[3] H. Guan, H. Shen, B. Jiao, Xu Wang, Mater. Sci. Semicond. Process. 25 (2014) 159–162.
[4] X. Meng, H. Deng, J. He, L. Sun, P. Yang, J. Mater. Lett. 151 (2015) 61–63.
[5] X. Zhang, N. Bao, K. Ramasamy, Y.A. Wang, Y. Wang, B. Lin, A. Gupta, Chem. Commun. 48 (2012) 4956–4958.
[6] Y. Li, T.F. Yuan, L.X. Jiang, Z.H. Su, F.Y. Liu, J. Alloys Comp. 610 (2014) 331–336.
[7] L. Li, B.L. Zhang, M. Cao, Y. Sun, J.C. Jiang, P.F. Hu, Y. Shen, J. Alloys Comp. 551 (2013) 24–29.
[8] F. Ozel, M. Kus, A. Yar, E. Arkan, M. Can, A. Aljabour, N.M. Varal, M. Ersoz, J. Mater. Sci. 50 (2015) 777–783.
[9] G. Rajesh, N. Muthukumarasamy, E.P. Subramaniam, S. Agilan, D. Velauthapillai, J. Sol-Gel Sci. Technol. 66 (2013) 288–292.
[10] M. Sabet, M.S. Niasari, D. Ghanbari, O. Amiri, M. Yousefi, Mater. Sci. Semicond. Process. 16 (2013) 696–704.
[11] S.M.H. Mashkani, F. Mohandes, M.S. Niasari, K.V. Rao, Mater. Res. Bull. 47 (2012) 3148–3159.
[12] G. Chen, J. Li, S. Chen, Z. Huang, M. Wu, Mater. Chem. Phys. 188 (2017) 95–99.
[13] P. Baláž, Mechanochemistry in Nanoscience and Minerals Engineering, Springer, Berlin Heidelberg, 2008, p. 413.
[14] P. Baláž, M. Achimovičová, M. Baláž, P. Billik, Z. Cherkezova-Zheleva, J.M. Criado, F. Delogu, E. Dutková, E. Gaffet, F.J. Gotor, R. Kumar, I. Mitov, T. Rojac, M. Senna, A. Streletskii, K. Wieczorek-Ciurowa, Chem. Soc. Rev. 42 (2013) 7571–7637.
[15] P. Baláž, M. Baláž, M.J. Sayagués, I. Škorvánek, A. Zorkovská, E. Dutková, J. Briančin, J. Kováč, J. Kováč Jr, Y. Shpotyuk, Nanoscale Res. Lett. 12 (2017) 256–266.
[16] P. Baláž, M. Baláž, A. Zorkovská, I. Škorvánek, Z. Bujnáková, J. Trajić, Acta Phys. Polon. 131 (4) (2017) 1153–1155.
[17] C. Yan, C. Huang, J. Yang, F. Liu, J. Liu, Y. Lai, J. Li, Y. Liu, Chem. Commun. 48 (2012) 2603–2605.
[18] T. Gürel, C. Sevik, T. Cagin, Phys. Rev. B 84 (2011) 205201.
[19] R.J. Gonzalez, R. Zallen, H. Berger, Phys. Rev. B 55 (11) (1997) 7014–7017.
[20] M. Himmrich, H. Haeuseler, Spectrochim. Acta 47A (7) (1991) 933–942.
[21] J.E. Spanier, I.P. Herman, Phys. Rev. B 61 (15) (2000) 10437.
[22] J.J. Saarinen, E.M. Vartiainen, K.E. Peiponen, Opt. Rev. 10 (2) (2003) 111.
[23] J.C.M. Garnett, Transaction of the Royal Society CCIII 385420, 1904.
[24] A. Saviola, I. Lindell, Dielectric Properties of Heterogeneous Materials PIER 6 Progres in Electromagnetic Research ed. A. Priou, Amsterdam, Elsevier, 1992, pp. 101–151.
[25] J.M. Chamberlain, P.M. Nikolic, M. Merda, P. Mihailovic, J. Phys. C: Solid State Phys. 9 (1976) L637–L642.
[26] G.P. Bernardini, P. Bonazzi, M. Corazza, F. Corsini, G. Mazzetti, L. Poggi, G. Tanelli, Eur. J. Mineral. 2 (1990) 219–225.
[27] Y. El Mendili, B. Minisini, A. Abdelouas, J.-F. Bardeau, RSC Adv. 4 (2014) 25827–25834.
[28] X. Fontané, V. Izquierdo-Roca, E. Saucedo, S. Schorr, V.O. Yukhymchuk, M.Ya. Valakh, A. Pérez-Rodríguez, J.R. Morante, J. Alloys Comp. 539 (2012) 190–194.